Cancer-Selective Targeting and Cytotoxicity by Liposomal-Coupled Lysosomal Saposin C Protein

Xiaoyang Qi,[1] Zhengtao Chu,[1] Yonatan Y. Mahller,[2] Keith F. Stringer,[3] David P. Witte,[3] and Timothy P. Cripe[2]

Abstract

Purpose: Saposin C is a multifunctional protein known to activate lysosomal enzymes and induce membrane fusion in an acidic environment. Excessive accumulation of lipid-coupled saposin C in lysosomes is cytotoxic. Because neoplasms generate an acidic microenvironment, caused by leakage of lysosomal enzymes and hypoxia, we hypothesized that saposin C may be an effective anticancer agent. We investigated the antitumor efficacy and systemic biodistribution of nanovesicles comprised of saposin C coupled with dioleoylphosphatidylserine in preclinical cancer models.

Experimental Design: Neuroblastoma, malignant peripheral nerve sheath tumor and, breast cancer cells were treated with saposin C–dioleoylphosphatidylserine nanovesicles and assessed for cell viability, ceramide elevation, caspase activation, and apoptosis. Fluorescently labeled saposin C–dioleoylphosphatidylserine was i.v. injected to determine *in vivo* tumor-targeting specificity. Antitumor activity and toxicity profile of saposin C–dioleoylphosphatidylserine were evaluated in xenograft models.

Results: Saposin C–dioleoylphosphatidylserine nanovesicles, with a mean diameter of ~190 nm, showed specific tumor-targeting activity shown through *in vivo* imaging. Following i.v. administration, saposin C–dioleoylphosphatidylserine nanovesicles preferentially accumulated in tumor vessels and cells in tumor-bearing mice. Saposin C–dioleoylphosphatidylserine induced apoptosis in multiple cancer cell types while sparing normal cells and tissues. The mechanism of saposin C–dioleoylphosphatidylserine induction of apoptosis was determined to be in part through elevation of intracellular ceramides, followed by caspase activation. In *in vivo* models, saposin C–dioleoylphosphatidylserine nanovesicles significantly inhibited growth of preclinical xenografts of neuroblastoma and malignant peripheral nerve sheath tumor. I.v. dosing of saposin C–dioleoylphosphatidylserine showed no toxic effects in nontumor tissues.

Conclusions: Saposin C–dioleoylphosphatidylserine nanovesicles offer promise as a novel, nontoxic, cancer-targeted, antitumor agent for treating a broad range of cancers. (Clin Cancer Res 2009;15(18):5840–51)

Saposins are small nonenzymatic glycoproteins present in all normal tissues that act as biological activators of lysosomal enzymes (1). These proteins are remarkably heat stable and protease resistant and contain an *N*-glycosylation consensus sequence and six essential cysteines (1, 2). Although the *N*-linked glycosylation is not essential for saposin C activity (2, 3), the functional organization of saposin C presents a membrane fusogenic domain and a region for activation of lysosomal enzymes (4, 5). Saposin C enhances degradation of glucosylceramide, sphingomyelin, and galactosylceramide to ceramide through acid β-glucosidase, acid sphingomyelinase, and acid β-galacotsylceramidase, respectively (1, 6, 7). In patients with lysosomal storage diseases, saposin C accumulates with glycosphingolipids in macrophages (8), and some have hypothesized that excessive saposin C and lipids may be toxic for these cells. Saposin B is a saposin family member that plays biological roles in degradation of sulfatide and membrane reorganizations (1).

Authors' Affiliations: Divisions of [1]Human Genetics, [2]Hematology/Oncology, and [3]Pathology, Department of Pediatrics, Cincinnati Children's Hospital Medical Center, University of Cincinnati College of Medicine, Cincinnati, Ohio

Received 12/22/08; revised 5/18/09; accepted 5/19/09; published OnlineFirst 9/8/09.

Grant support: CancerFree Kids, Translational Research Initiative and Validation Research Grants from Cincinnati Children's Hospital Medical Center (X. Qi). The costs of publication of this article were defrayed in part by the payment of page charges. This article must therefore be hereby marked *advertisement* in accordance with 18 U.S.C. Section 1734 solely to indicate this fact.

Note: Supplementary data for this article are available at Clinical Cancer Research Online (http://clincancerres.aacrjournals.org/).

Patents are pending for the intellectual property disclosed in this article.

Requests for reprints: Xiaoyang Qi, Division and Program in Human Genetics, 3333 Burnet Avenue, Cincinnati, Ohio 45229-3039. Phone: 513-636-5964; Fax: 513-636-3486; E-mail: xiaoyang.qi@cchmc.org.

doi:10.1158/1078-0432.CCR-08-3285

Translational Relevance

Small lysosomal protein saposin C and the phospholipid dioleoylphosphatidylserine assemble into stable saposin C–dioleoylphosphatidylserine nanovesicles. We found that these nanovesicles have remarkable cancer-selective targeting and cytotoxicity for multiple types of cancer cells. Saposin C–dioleoylphosphatidylserine nanovesicles killed cancer cells by inducing apoptosis, whereas untransformed cells (controls) remained unaffected. *In vitro* studies, using neuroblastoma cells, revealed that saposin C–dioleoylphosphatidylserine induced ceramide elevation, followed by caspase activation. *In vivo*, saposin C–dioleoylphosphatidylserine showed strong antitumor effects in xenograft mouse models of human neuroblastoma and malignant peripheral nerve sheath tumors. In addition, saposin C–dioleoylphosphatidylserine had no significant toxic effects in mice. Our findings suggest that saposin C–dioleoylphosphatidylserine nanovesicles are a feasible and nontoxic novel anticancer therapeutic.

A general property of saposins is their lipid membrane binding activity (9) because they play important roles in lipid transport (10), lipid microdomain assembly (11), and reorganization of biological membranes (12–14). Specifically, saposin C associates with lipid membranes by embedding into membrane leaflets. Each helical peptide of saposin C at the amino and carboxyl ends of the molecule is essential for insertion into lipid bilayers (9). Saposin C preferentially interacts with unsaturated, negatively charged phospholipids (such as dioleoylphosphatidylserine) at acidic pH (5, 9). This interaction is required for saposin C activation of lysosomal enzymes. We hypothesized that, because phosphatidylserine is relatively abundant on the surface of tumor tissues (15, 16), it would provide a tumor-specific target for saposin C. In comparison with untransformed cells, neoplastic cells are hypermetabolic and thus produce significant amounts of acid and carbon dioxide as by-products of anaerobic glycolysis and aerobic respiration, respectively. Hydrogen ions accumulate in tumor tissues, and as a result, the mean extracellular pH in solid tumors is lower (pH ~6) than that in normal tissues (pH ~7; refs. 17, 18). Cancerous cells also display other unique properties such as generalized membrane alterations (19–21) and "leakiness" of lysosomal enzymes (19). Intriguingly, several lysosomal hydrolases have been found elevated in tumor tissues (22, 23). Therefore, a unique acidic microenvironment with extracellular leakage of lysosomal enzymes makes tumor tissue an optimal target for saposin C.

In the last two decades, cellular membranes have become targets for anticancer drugs (24, 25). Several lines of evidence have suggested a linkage between cellular membrane abnormalities and ceramide-mediated induction of apoptosis in tumors (26–29). Based on these observations, agents that interfere with cellular membranes have been developed to modulate membrane organization, fluidity, metabolism, and signal transduction (24, 25). Little is known however of the underlying signaling pathways affected by membrane-targeted antineoplastic agents. The *in vivo* antitumor efficacy and tumor-targeting ability of such agents is entirely lacking or suboptimal.

Extracranial neural tumors remain a significant clinical challenge despite aggressive multimodal therapy (30). Pediatric neuroblastoma is the most common extracranial solid tumor of childhood (31), and malignant peripheral nerve sheath tumors are the major cause of mortality in patients with neurofibromatosis type 1 (32). Multidrug resistance is frequently observed in neuroblastoma and malignant peripheral nerve sheath tumor, and many patients with high-risk disease undergo relapse (33, 34). Similarly, conventional therapies are ineffective for patients with malignant peripheral nerve sheath tumor (35). Surgical resection is often the only effective form of treatment but is not often feasible. Therefore, these patients represent major unmet medical needs in neuroblastomas and malignant peripheral nerve sheath tumor.

In the current article, we show the anticancer utility of a novel therapeutic, saposin C–dioleoylphosphatidylserine. We describe saposin C–dioleoylphosphatidylserine nanovesicle formation, characterization, *in vivo* tumor targeting, and antineoplastic activity against human tumor cells and xenografts. We also investigated the mechanism behind saposin C–dioleoylphosphatidylserine–mediated antitumor activity. Finally, we evaluated the preclinical safety of this novel therapeutic against untransformed cells and in mouse models.

Materials and Methods

Cell culture and mouse xenografts. Human breast cancer (MCF-7), human breast (MCF-10A), and human normal fibroblast (HNF) cells were from American Type Culture Collection and grown in DMEM with 10% fetal bovine serum. Human neuroblastoma cells (CHLA-20 -79, -90, -172, SK-SY-5Y) were gift from gifts from Thomas Inge (Cincinnati Children's Hospital Medical Center) and Robert Seeger (Children's Hospital of Los Angeles); their origins and culture conditions have been described (36). Human malignant peripheral nerve sheath tumor cells (STS26T and S462) were kindly provided by Jeff DeClue (National Cancer Institute) and Nancy Ratner (Cincinnati Children's Hospital), and cultured as previously described (36). Cells were cultured at 37°C in 5% CO_2. Neuroblastoma cells and tumors were confirmed by immunohistochemistry analysis using rabbit anti-human synaptophysin (Dako) or mouse anti–human neuron–specific enolase (Cell Marque), according to the manufacturers' instructions. (data not shown). Characterization of malignant peripheral nerve sheath tumor cells were done as previously described (36). No cross-contamination was found in these cells and xenografted tumors.

N4 plus particle size analyzer, transmission electron microscopy, and fluorescence spectroscopic analysis. Nanovesicle size was determined by photon correlation spectroscopy using an N4 plus particle size analyzer (Coulter). Transmission electron microscopy images were taken with a Hitachi transmission electron microscopy (H-7600; Hitachi) operated at an acceleration voltage of 80 kV. Tryptophan fluorescence spectroscopic analysis was carried out as previously reported (9).

Preparation of proteins and nanovesicles. Saposin proteins were produced as previously described (2). Briefly, recombinant saposins were expressed using the pET system in *Escherichia coli* cells. Expressed proteins contained a His-tag and were purified on a nickel column and completely desalted with C4 reverse-phase high performance liquid chromatography chromatography. After lyophilization, saposin powder was used, and its concentration was determined by its weight. All phospholipids were purchased from Avanti Polar Lipids. Bath sonication was used to form saposin C–dioleoylphosphatidylserine or saposin B–dioleoylphosphatidylserine nanovesicles, as previously described with minor modification (37). After solvent removal under nitrogen gas, phospholipids were mixed with pure saposin proteins in 20 μL of acid buffer (pH 5) and quickly diluted in 50× volume of physiologic aqueous solu-

tion. The protein-lipid mixture was then gently sonicated, and the two components readily assembled into nanovesicles. Once formed, saposin C–dioleoylphosphatidylserine nanovesicles were monitored by a N4 plus subsize particle size analyzer. Saposin B–dioleoylphosphatidylserine was used in control experiments. Saposin C binds the lipid molecules and spontaneously incorporates into the lipid bilayer of the liposomes upon sonication. Following sonication and ultracentrifugation to pellet saposin C–dioleoylphosphatidylserine coupled liposomes, no detectable saposin C was detected in the supernatant fraction, implicating a very high loading/coupling efficiency.

Preparation of fluorescently labeled saposin C–dioleoylphosphatidylserine nanovesicles and saposin C. An aliquot of CellVue Maroon (PTI Research, Inc.) in ethanol was mixed with phospholipid solvent for bath sonication preparation by the procedure, as described above. CellVue Maroon–labeled saposin C–dioleoylphosphatidylserine nanovesicle had an excitation maximum at 653 nm and an emission maximum at 677 nm (Supplemental Fig. S1D). Fluorescent saposin C was labeled using Alexa Flour 660 amine-react probe kit, according to the manufacturer's suggested labeling protocol (Invitrogen). CellVue Maroon–labeled saposin C–dioleoylphosphatidylserine nanovesicles or fluorescent saposin C were separated from free CellVue Maroon dye or Alexa Fluo probe using a Sephadex G25 column (PD-10; Amersham Pharmacia Biotech).

Cell viability assay. Viable cell density was assessed by MTT assay (Sigma). Cells were seeded at a density of 10^4 cells in each well of a 96-well, flat-bottom tissue culture plate (Falcon, Becton Dickson Labware) in 100 μL of complete medium with or without saposin C–dioleoylphosphatidylserine. MTT assays were done as previously described (36).

Ultracentrifugation and Western blot. To evaluate the tight binding of saposin and phospholipid membrane in nanovesicles, ultracentrifugation was used to separate nanovesicle particles from free saposins. Ultracentrifugation was done using a Bakeman XL-90 centrifuge with a SW55TI rotor. Saposin C–dioleoylphosphatidylserine solution was centrifuged at high speed (300,000 rpm) for 3 h at 4°C. Western blot was done using NuPAGE Novex Bis-Tris Gels (4-12%) and the electrophoresis procedure per manufacturer (Invitrogen). Protein was transferred using a Semi-Dry blotting unit (FB-SDB-2020; Fisher Biotech) to Hybond-ECL Nitrocellulose membrane (Amersham Biosciences). Rabbit anti-human saposin C polyclonal antibody and secondary mouse horseradish peroxidase–conjugated were used for saposin C detection. Anti–human caspase-3 and caspase-9 antibodies (Cell Signaling Technology) were used for detection of active caspases.

In vivo *tumor xenografts and treatments.* Human neuroblastoma cells (CHLA-20; 7.5×10^6) were injected s.c. into the upper back of 4- to 6-wk-old female athymic nude mice (Taconic). Tumor volumes were estimated according to the formula $V = (\pi/6)LW^2$ (V, volume; L, length; W, width). The data represent the mean ± SE ($n = 10$) in each group. On day 28 postimplantation, when the mean tumor volume was ~150 to 200 mm^3, animals were randomized into two groups. Animals were administered either saposin C–dioleoylphosphatidylserine nanovesicles or dioleoylphosphatidylserine alone by tail-vein injection. Animals received four treatments given 3 d apart. In a second experimental model, 3×10^6 human malignant peripheral nerve sheath tumor cells (STS26T) were injected i.p. into 6- to 8-wk-old female athymic mice (Harlan). At day 7 postinoculation, mice ($n = 7$ per group) were treated with saposin C–dioleoylphosphatidylserine or PBS by i.p. injection. Animals received six treatments given 3 d apart. Mice were followed for gross tumor burden for a period of 18 d, at which time animals were euthanized and their tumor harvested and quantified.

In vitro *and* in vivo *tumor targeting of the CellVue Maroon–labeled saposin C–dioleoylphosphatidylserine nanovesicles.* For *in vitro* experiments, CellVue Maroon–labeled saposin C–dioleoylphosphatidylserine (200 μL; saposin C, 100 μmol/L; dioleoylphosphatidylserine, 260 μmol/L; CellVue Maroon, 40 μmol/L) was incubated with live cells for 12 h. Fluorescence photographs were taken with a Zeiss Axiovert 200 microscope equipped with Axiovision (4.3) software (Zeiss) and filters for Cy5 and 4′,6-diamidino-2-phenylindole. For *in vivo* imaging, CellVue Maroon–labeled saposin C–dioleoylphosphatidylserine, saposin C and CMV-labeled dioleoylphosphatidylserine, or CellVue Maroon–labeled dioleoylphosphatidylserine alone were administrated by tail vein into mice bearing s.c. neuroblastoma xenografts. Real-time images were taken using an IVIS 200 Series imaging system with an XFO-6 fluorescent kit (Xenogen).

Immunofluorescence analysis. Immunofluorescence microscopy was done with sections prepared from frozen-embedded tumors. After blocking in diluted donkey and goat sera, rat anti-CD31 antibody (BD Bioscience Pharmingen), chicken anti–His-tag antibody (Novus Biologicals), and/or rabbit anti-saposin C were incubated (1:200) overnight at 4°C. After washing, sections were developed using biotinylated donkey anti-rat, biotinylated donkey anti-chicken, and/or Alexa Fluor 488– or 594–labeled goat anti-rabbit secondary antibodies for 30 min at room temperature. After subsequent washing, biotinylated antibody was detected with Alexa Fluor 594–labeled avidin conjugate (Molecular Probes). After cover slips were placed, sections were photographed with a Spot RT Slider digital camera (Diagnostic Instruments) using a fluorescence microscope equipped with blue, green, and red filter sets (Nikon Instruments).

In vitro *and* in vivo *terminal deoxynucleotidyl transferase–mediated dUTP nick end labeling (TUNEL) assay for apoptosis.* *In vitro* apoptosis induction was determined by TUNEL assay, using an *In situ* Cell Death Detection Kit, horse-radish peroxidase (POD) (Roche Applied Science). Experiments were carried out per manufacture's protocol. After substrate reaction, stained apoptotic cells were counted under a fluorescence microscope (Zeiss Axiovert 200) with a fluorescein isothiocyanate filter. Cells were labeled with red fluorophore propidium iodide to determine total cell numbers in the field of view. *In vivo* TUNEL assay was done on frozen tissue sections from neuroblastoma xenografts after treatment with saposin C–dioleoylphosphatidylserine or PBS 50 h postinjection.

In vitro *caspase activity assay.* Caspase activity in saposin C–dioleoylphosphatidylserine–treated cells was measured using a Caspase Protease Assay Kit, following manufacture's protocols (BioSource International). Comparison of the absorbance of pNA from saposin C–dioleoylphosphatidylserine–treated and nontreated samples allowed determination of the fold changes in activity of caspase-3, caspase-8, and caspase-9.

Acid sphingomyelinase assay. Cells were lysed by three cycles of freeze and thawing in lysis buffer (50 mmol/L sodium acetate; pH 5.0). The lysate was centrifuged at 10,000 × *g* at 4°C for 10 min. The supernatant was used to assay acid sphingomyelinase activity, as described by Liu and Hannun (38) using [*N*-methyl-^{14}C]sphingomyelin (2.0 GBq/mmol; GE Healthcare) as the substrate with slight modification. Supernatant protein (50 μg) was mixed in a reaction mixture (20 mmol/L sodium acetate, pH 5.0; 5 nmol of dioleoylphosphatidylserine; 5 nmol [*N*-methyl-^{14}C] sphingomyelin; and 0.1% Triton X-100) and incubated at 37°C for 2 h. The reaction was stopped by adding 1.5 mL of chloroform:methanol (v/v, 2:1) and 0.2 mL of water; the upper aqueous phase was removed and mixed with 5 mL of scintillation cocktail for counting. Specific activity of acid sphingomyelinase was expressed as nanomoles of substrate hydrolyzed per milligram protein per hour.

Quantification of ceramides and sphingosine bases. Ceramides and sphingosine bases in saposin C–dioleoylphosphatidylserine–treated cells were measured using liquid chromatography–mass spectrometry method at lipidomics core of the Medical University of South Carolina (39). The cells (2×10^6 cells) were scraped with ice-cold PBS and pelleted by centrifugation at 1000 rpm for 5 min. The cell pellets were used for lipid extract and analysis by the core, as described previously (39). The analysis was done on a Thermo Finnigan TSQ 7000 triple quadrupole mass spectrometer operating in a Multiple Reaction Monitoring positive ionization mode. Peaks for the target analytes and internal standards were collected and processed using the Xcalibur software system (Xcalibur Software, Inc.). Calibration curves were constructed by plotting peak area ratios of synthetic standards representing each target analyte to the corresponding internal standard. Ceramide was analyzed by the diacylglycerol kinase method, as described (40). Briefly, lipids extracted from cell pellet (1×10^6 cells) in chloroform:methanol (v/v, 1:2) were incubated at room temperature for 30 min with β-octylglucoside/dioleoylphosphatidyl glycerol micelles, 5 μg diacylglycerol kinase,

2 mmol/L dithiothreitol, and 2 μCi [γ-^{32}P]ATP in a final volume of 80 μL. The reaction was stopped by the addition of 1.5 mL of chloroform: methanol (v/v, 1:2), 0.3 mL of water, 0.5 mL of chloroform, and 0.5 mL of 1% perchloric acid. The samples were centrifuged at 2,000 × *g* for 5 min. The lower phase was collected and dried for TLC. [^{32}P]Ceramide-1-phosphate was separated on TLC plates (Whatman Silica Gel 60A, Whatman) with the solvent system containing chloroform:acetone: methanol:acetic acid:water (v/v, 10:4:3:2:1). Radiolabeled ceramide was visualized using the phosphorimager (Storm 860, Molecular Dynamics). The amounts of ceramide was quantified by scraping the bands and counting with a scintillation counter.

Data analysis. MTT experiments were done in quadruplicate, and data were analyzed by ANOVA. The data presented are the arithmetic mean ± SE. *t* Test analysis or two-way ANOVA Tukey test were used to determine statistical significance for experiments with two or greater than two groups, respectively. Analyses were done with SPSS 12.0.

Results

Preparation and characterization of saposin C–dioleoylphosphatidylserine nanovesicles. Saposin C–dioleoylphosphatidylserine nanovesicles were formed at acidic pH using bath sonication, as described in the Methods. Saposin C–coupled dioleoylphosphatidylserine liposomes remained intact for 3 days at room temperature by monitoring using a N4 plus particle size analyzer (data not shown). Saposins have previously been shown to be thermotolerant and resistant to sonication (1, 2). To determine the coupling efficiency of saposin C with dioleoylphosphatidylserine, we did ultracentrifugation to pellet intact vesicles. Following ultracentrifugation of a saposin C–dioleoylphosphatidylserine suspension, saposin C was found in the pellet fraction and not in the supernatant (Supplementary Fig. S1A, *lanes 1* and *2*). Addition of neutral pH buffer caused saposin C to localize to the supernatant fraction (*lanes 3* and *4*). To address the possibility that free saposin C may pellet at acidic pH, we showed that, in the absence of dioleoylphosphatidylserine, saposin C remains in the supernatant (*lanes 5* and *6*). An N4 plus particle size analyzer revealed that sonicated saposin C–dioleoylphosphatidylserine complexes contained monodispersed vesicles with a mean diameter of ~190 nm (Supplementary Fig. S1B). Transmission electron microscopy analysis illustrated unilamellar saposin C–dioleoylphosphatidylserine vesicles (Supplementary Fig. S1B, *inset*). Protein and lipid membrane association in saposin C–dioleoylphosphatidylserine was further confirmed by a tryptophan fluorescence spectroscopy. Because saposin C is a tryptophan-free protein, tryptophan was introduced into saposin C (0 W) by site-directed mutagenesis (9). When saposin C (0 W) and dioleoylphosphatidylserine formed nanovesicles, a blue shift was observed in saposin C (0 W) tryptophan fluorescence, indicating membrane insertion (Supplementary Fig. S1C; ref. 9).

Antineoplastic effect of saposin C–dioleoylphosphatidylserine by induction of apoptotic cell death. Cytotoxicity due to saposin C through lipid accumulation inside cells from patients with lysosomal storage disease led us to hypothesize that exogenously loaded saposin C–lipid complexes may have cytotoxic effects against human cancer cells. First, we determined the optimal molar ratio of saposin C and dioleoylphosphatidylserine for maximal cytotoxic effect against human neuroblastoma (CHLA-20) cells. The optimal ratios were found from 1:3 to 1:7 (Fig. 1A). Incubation of human neuroblastoma and malignant peripheral nerve sheath tumor cells with coupled saposin C–dioleoylphosphatidylserine led to a dramatic alteration of cell morphology, including membrane blebbing, chromatin condensation, and inhibition of cell growth (Supplementary Figs. S2A and B). Cell viability assays revealed that saposin C–dioleoylphosphatidylserine inhibits >90% growth of human neuroblastoma (CHLA-20 and -79), malignant peripheral nerve sheath tumor (S462 and STS26T), and breast cancer (MCF-7) cells but has no significant inhibitory effect on nontransformed cells (MCF-10A and HFC; Fig. 1B). The half maximal inhibitory concentration (IC_{50}) values were estimated using sigmoidal dose-response equation (GraphPad, Prism). At 1:3 (saposin C: dioleoylphosphatidylserine) molar ratio, saposin C–dioleoylphosphatidylserine showed IC_{50} of 77.8, 37.8, 37.2, 149.12, and 154.4 μmol/L for CHLA-20, CHLA-79, S462, STS26T, and MCF-7, respectively. We further investigated if the observed cytotoxic effect required coupling of saposin C and dioleoylphosphatidylserine. Dioleoylphosphatidylserine or saposin C showed no or less inhibitory effects on cancer cell growth (Fig. 1C and D; Supplementary Fig. S2A). In addition, no significant cytotoxic effect on CHLA-20 cells was observed with coaddition of uncoupled saposin C and dioleoylphosphatidylserine (Supplementary Fig. S3A). To determine if the observed cytotoxic effect was specific for saposin C, we evaluated another saposin family protein, saposin B, coupled with dioleoylphosphatidylserine. Coupled saposin B–dioleoylphosphatidylserine showed no effect upon proliferation (Supplementary Fig. S3A). These data indicate that the observed cytotoxic effect is specific for saposin C and requires coupled saposin C–dioleoylphosphatidylserine nanovesicles.

Untransformed human mammary (MCF-10A) and fibroblast cell lines (HFC) treated with saposin C–dioleoylphosphatidylserine showed proliferation on par with mock controls, suggesting that saposin C–dioleoylphosphatidylserine is not toxic for untransformed cells (Fig. 1B). Because mutation of p53 is found in >70% of cancer cells, we sought to determine if treatment with saposin C–dioleoylphosphatidylserine was toxic for such cells. We showed that saposin C–dioleoylphosphatidylserine is cytotoxic against $p53^{-/-}$ cancer cells (CHLA-90 and CHLA-172), suggesting that saposin C–dioleoylphosphatidylserine cytotoxicity is not p53 dependent (Supplementary Fig. S3B). We also observed that MCF-7 cells, which possess a dominant negative caspase-9 mutation, were not affected by saposin C–dioleoylphosphatidylserine (Supplementary Fig. S3C). Supporting this finding, saposin C–dioleoylphosphatidylserine mediated cytotoxicity was substantially reduced following transfection of cancer cells with dominant negative caspase-9. Therefore, the cytotoxic effect of saposin C–dioleoylphosphatidylserine seems tumor-selective and to be mediated through caspase-9.

Induction of apoptosis by saposin C–dioleoylphosphatidylserine, as revealed by TUNEL assay, was dose and time dependent (Fig. 2A-C). The most potent apoptosis inducing dose was observed at 40 μmol/L saposin C and 120 μmol/L dioleoylphosphatidylserine, and the peak apoptotic effect was observed between 48 and 53 hours. Similar results were seen with cell lines CHLA-79 and SK-N-SH (data not shown).

Saposin C–dioleoylphosphatidylserine induced ceramide elevation and activated caspases. We hypothesized that saposin C–dioleoylphosphatidylserine induced apoptosis was mediated in part through elevation and accumulation of ceramide and downstream activation of caspases (Fig. 3A). To test this hypothesis, we quantified ceramide concentration and caspase levels in cancer cells treated with saposin C–dioleoylphosphatidylserine

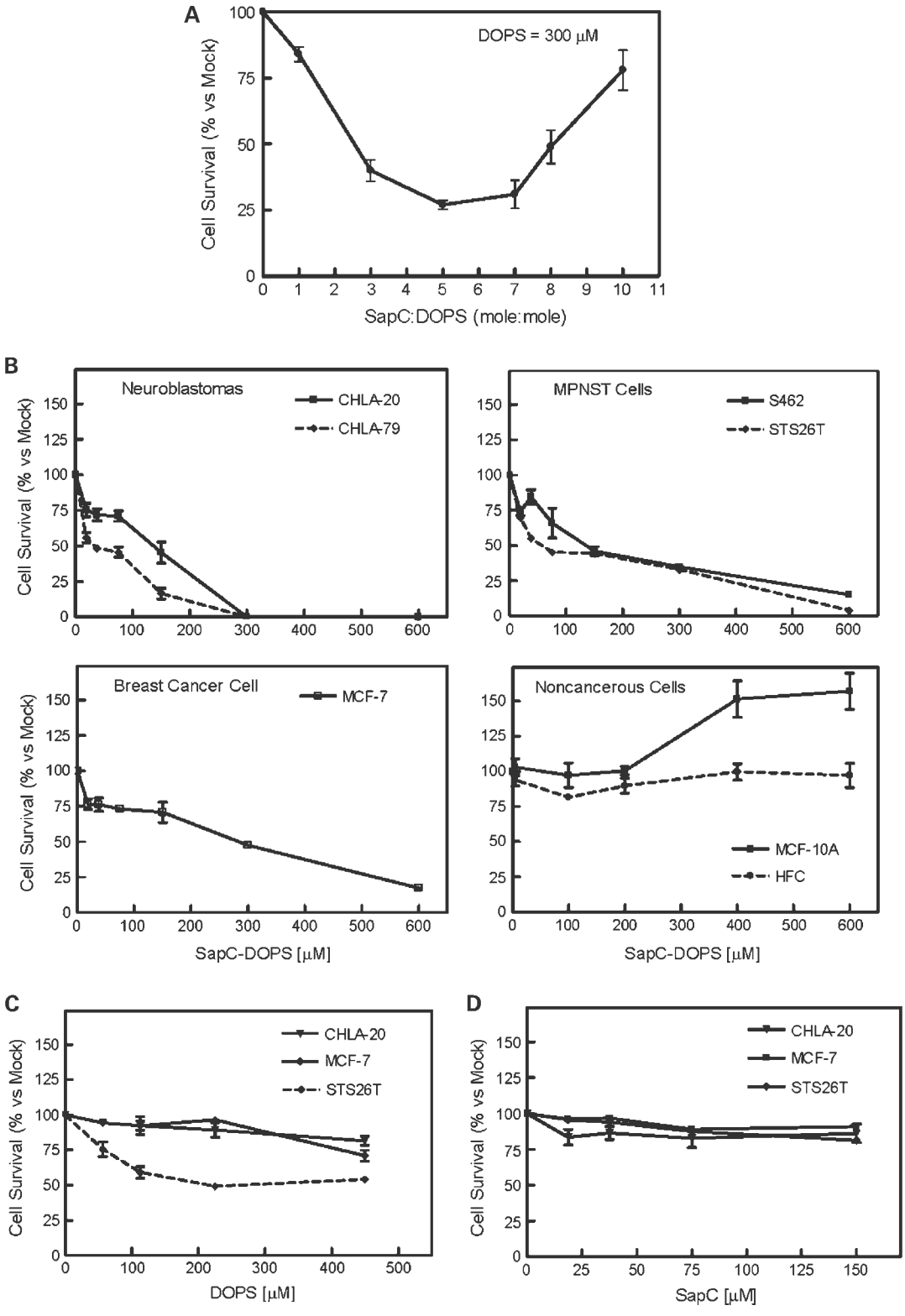

Fig. 1. Coupled saposin C–dioleoylphosphatidylserine is cytotoxic against human cancer cells. *A,* determination of optimal concentration of saposin C and dioleoylphosphatidylserine for maximal cytotoxic effect on human neuroblastoma (CHLA-20) cells. *B,* treatment of human neuroblastoma (CHLA-20 and -79), malignant peripheral nerve sheath tumor (S462 and STS26T), breast cancer (MCF-7), and noncancerous (MCF-10A and HFC) cells with coupled saposin C–dioleoylphosphatidylserine. *C,* treatment of CHLA-20, MCF-7, and STS26T cells with dioleoylphosphatidylserine alone or saposin C alone. Experimental conditions: cells (4×10^4/100 μL per well) were cultured for 24 h before the treatment. MTT assay was carried out after culture of the treated cells for 3 d. Spectrophotometric data from quadruplication wells (in 96-well plates) were analyzed by ANOVA. The data were presented as the arithmetic means ± SE. Experiments were done at least twice. Saposin C:dioleoylphosphatidylserine, 1:3 (mole:mole) in (*B* and *C*).

nanovesicles. Using liquid chromatography–mass spectrometry, we discovered that ceramide levels in saposin C–dioleoylphosphatidylserine treated human neuroblastoma cancer cells were dramatically increased 6-fold compared with controls (Fig. 3B). These results were confirmed by the diacylglycerol kinase method (Supplementary Fig. S4A and B). A major source of ceramide is the hydrolysis of membrane sphingomyelin to generate ceramide and phosphorylcholine by sphingomyelinase. We observed that saposin C–dioleoylphosphatidylserine treatment elevated acid sphingomyelinase activity in a dose-dependent manner in neuroblastoma (CHLA-20) and malignant peripheral nerve sheath tumor (STS26T) cells using radiolabeled sphingomyelin assay (Supplementary Fig. S5). We also found >5-fold elevated caspase levels in human neuroblastoma cells treated with saposin C–dioleoylphosphatidylserine in comparison with controls (Fig. 3C). A time-course analysis revealed that caspase-3, caspase-8, and caspase-9 activity reached peak levels after 48 to 53 hours incubation. Active cleaved caspases were increased in the presence of saposin C–dioleoylphosphatidylserine as shown by western blot but not significantly detected in controls (Fig. 3D).

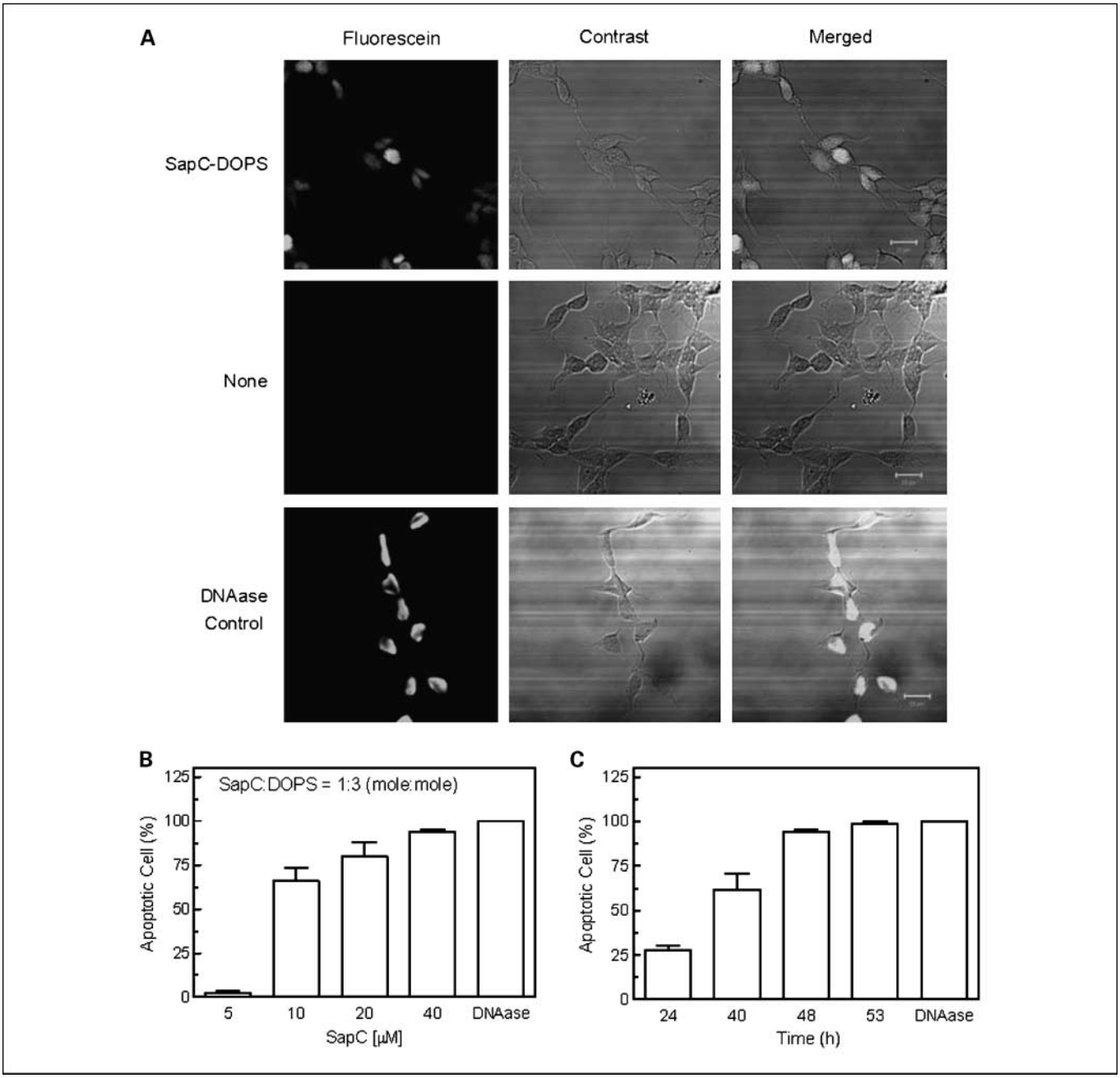

Fig. 2. TUNEL analysis of cells and tissue sections from human neuroblastoma (CHLA-20) xenografts. *A,* neuroblastoma cells (CHLA-20) were treated with saposin C–dioleoylphosphatidylserine or PBS for 30 h, collected, and stained with TUNEL stain followed by fluorescein to indicate apoptotic cells. DNase treated cells were used as a positive control. *B* and *C,* dose- and time-dependent induction of apoptosis by saposin C–dioleoylphosphatidylserine treatment as measured by TUNEL staining (DNase positive control).

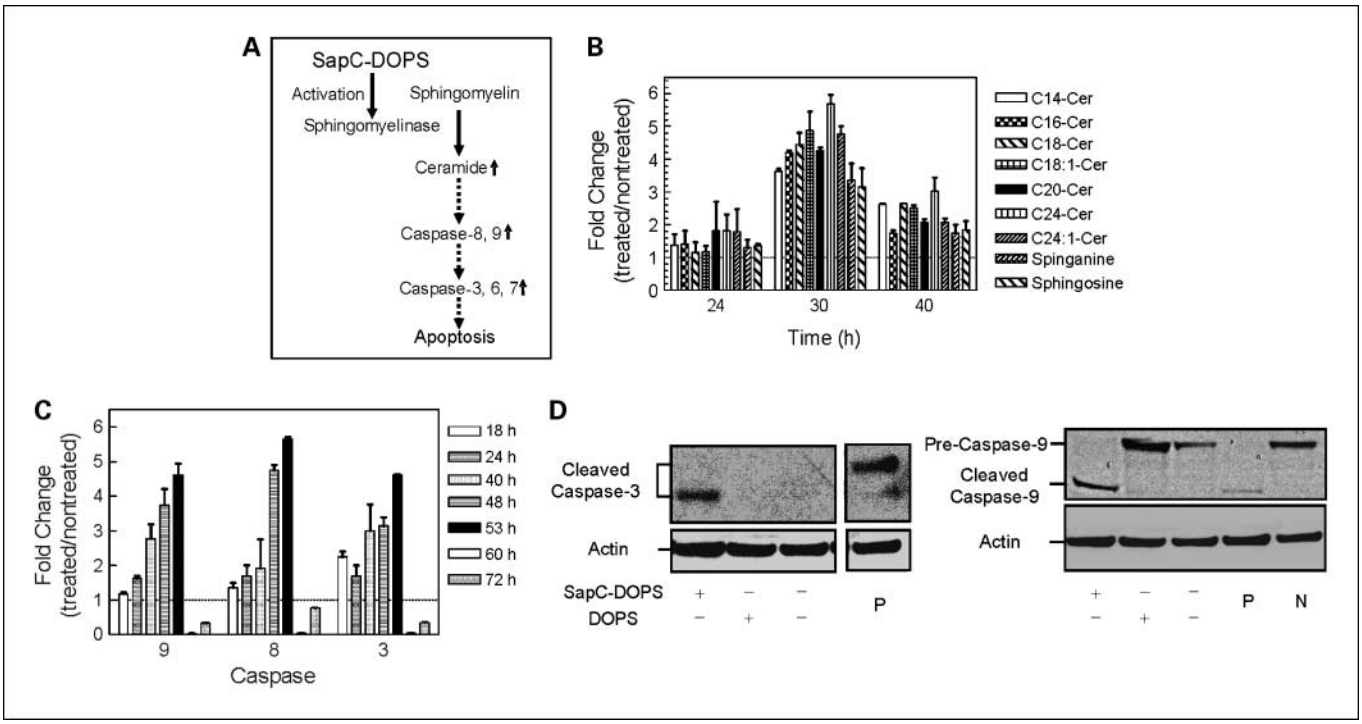

Fig. 3. Saposin C–dioleoylphosphatidylserine induced ceramide accumulation and caspase activation. *A,* schematic mechanism illustrating possible mechanism of saposin C–dioleoylphosphatidylserine mediated activation of cellular caspases. *B,* time course of ceramide accumulation induced by saposin C–dioleoylphosphatidylserine in CHLA-20 cells. *C,* time course of caspase-3, caspase-8, and caspase-9 activation by saposin C–dioleoylphosphatidylserine in CHLA-20 cells. The data are shown as fold above the untreated control at each time point. *D,* western blot determination of caspase activation by saposin C–dioleoylphosphatidylserine treatment. P, staurosporine positive control; N, negative control. Saposin C, 30 μmol/L; dioleoylphosphatidylserine, 300 μmol/L.

These findings suggest that saposin C–dioleoylphosphatidylserine may triggers ceramide elevation, caspase activation, and finally, apoptosis.

In vitro *and* in vivo *tumor targeting of saposin C–dioleoylphosphatidylserine nanovesicles.* Saposin C incorporated within dioleoylphosphatidylserine vesicles is capable of cell internalization by crossing cellular plasma membranes (37). To label saposin C–dioleoylphosphatidylserine nanovesicles, a lipophilic fluorescent probe, CellVue Maroon, was incorporated into lipid bilayers during nanovesicles preparation. Addition of the fluorophore did not alter nanovesicle formation (data not shown). Human neuroblastoma cells (CHLA-20) incubated with CellVue Maroon–labeled nanovesicles showed a strong fluorescent signal detected inside cells (Fig. 4A). This result indicated that CellVue Maroon–labeled saposin C–dioleoylphosphatidylserine could be incorporated into tumor cells.

In vivo biodistribution of CellVue Maroon–labeled saposin C–dioleoylphosphatidylserine was conducted in mice bearing human neuroblastoma xenografts using real-time fluorescence imaging. For these studies we evaluated i.v. injection of CellVue Maroon–labeled saposin C–dioleoylphosphatidylserine complexes (mouse 1), uncoupled saposin C and CellVue Maroon–labeled dioleoylphosphatidylserine vesicles (mouse 2), CellVue Maroon–labeled dioleoylphosphatidylserine alone (mouse 3) or PBS in a non–tumor bearing mouse (mouse 4; Fig. 4B). At early time points (0.5 and 5 hours) postinjection, fluorescent signal was detected in tumor and nontumor tissues (likely liver; Fig. 4B). However, by 12 hours postinjection, a fluorescent signal from tumor site was only observed in tumor-bearing mice that had received complexed saposin C–dioleoylphosphatidylserine (Fig. 4B, *mice 1* and *2*). In addition, at 12 hours, animals that received saposin C–dioleoylphosphatidylserine complexes had a significantly decreased fluorescent signal in nontumor sites compared with uncoupled saposin C and CMV-labeled dioleoylphosphatidylserine (Fig. 4B, *mouse 1* versus *mouse 2*). Animals receiving CellVue Maroon–labeled dioleoylphosphatidylserine alone showed minimal fluorescence distribution that was absent by 12 hours postinjection, likely because of the short half-life of dioleoylphosphatidylserine without saposin C (Fig. 4B, *mouse 3*). By 24 hours, animals receiving saposin C–dioleoylphosphatidylserine complexes still showed a fluorescent signal in tumor tissue, whereas those receiving uncoupled saposin C and CMV-labeled dioleoylphosphatidylserine only showed a fluorescent signal in the liver (Fig. 4B, mouse 2). Tumor fluorescence remained for at least 48 hours (Fig. 4B, *mouse 1*), sometimes up to 100 hours. Animals receiving uncoupled saposin C and CMV-labeled dioleoylphosphatidylserine showed no accumulation of fluorescence signal at 48 hours (Fig. 4B, mouse 2). Fluorescence immunohistochemistry revealed a strong CellVue Maroon signal in tumor cells and vessels from animals treated with CellVue Maroon–labeled saposin C–dioleoylphosphatidylserine but not in control tumors (Supplementary Fig. S6A, *a-c*). Identification of tumor and stroma vessels by CD31 staining indicated that only tumor vessels were positive for CellVue Maroon fluorescence (Supplementary Fig. S6A, *d-g*). In addition, saposin C was located in tumor tissues using anti-saposin C and anti–His-tag antibodies and not within adjacent stromal tissues (Supplementary Fig. S6A, *h-k*). Fluorescent signal of CellVue Maroon–labeled saposin C–dioleoylphosphatidylserine vesicles was detected in liver and spleen tissues of mice at early time

points, but by 24 hours postinjection, no signal was detected. In addition, uptake of saposin C in the liver and spleen was determined in tumor-bearing mice at 24 hours postinjection by Western blot analysis. No saposin C was detected using either anti–saposin C or anti–His-tag antibodies (Supplementary Fig. S6B). These results indicate that saposin C–dioleoylphosphatidylserine nanovesicles accumulate preferentially within tumor sites and that saposin C is essential for its tumor-targeting properties.

Because saposin C does not associate with CellVue Maroon dye, we could not do *in vivo* biodistribution studies with CellVue Maroon–labeled saposin C. To evaluate the tumor-targeting effect of saposin C alone, saposin C was labeled with a far-red fluorescent probe, Alexa Flour 660. No fluorescent signal was detected in tumor sites using the IVIS200 bioluminescence imaging system (Supplementary Fig. S7). These data suggest that saposin C alone has no readily detectable tumor-targeting property.

Tumor uptake of fluorescent-coupled saposin C–dioleoylphosphatidylserine nanovesicles was determined in neuroblastoma xenografts. To confirm the validity of our approach, *in vivo* imaging of intratumorally injected CellVue Maroon–labeled

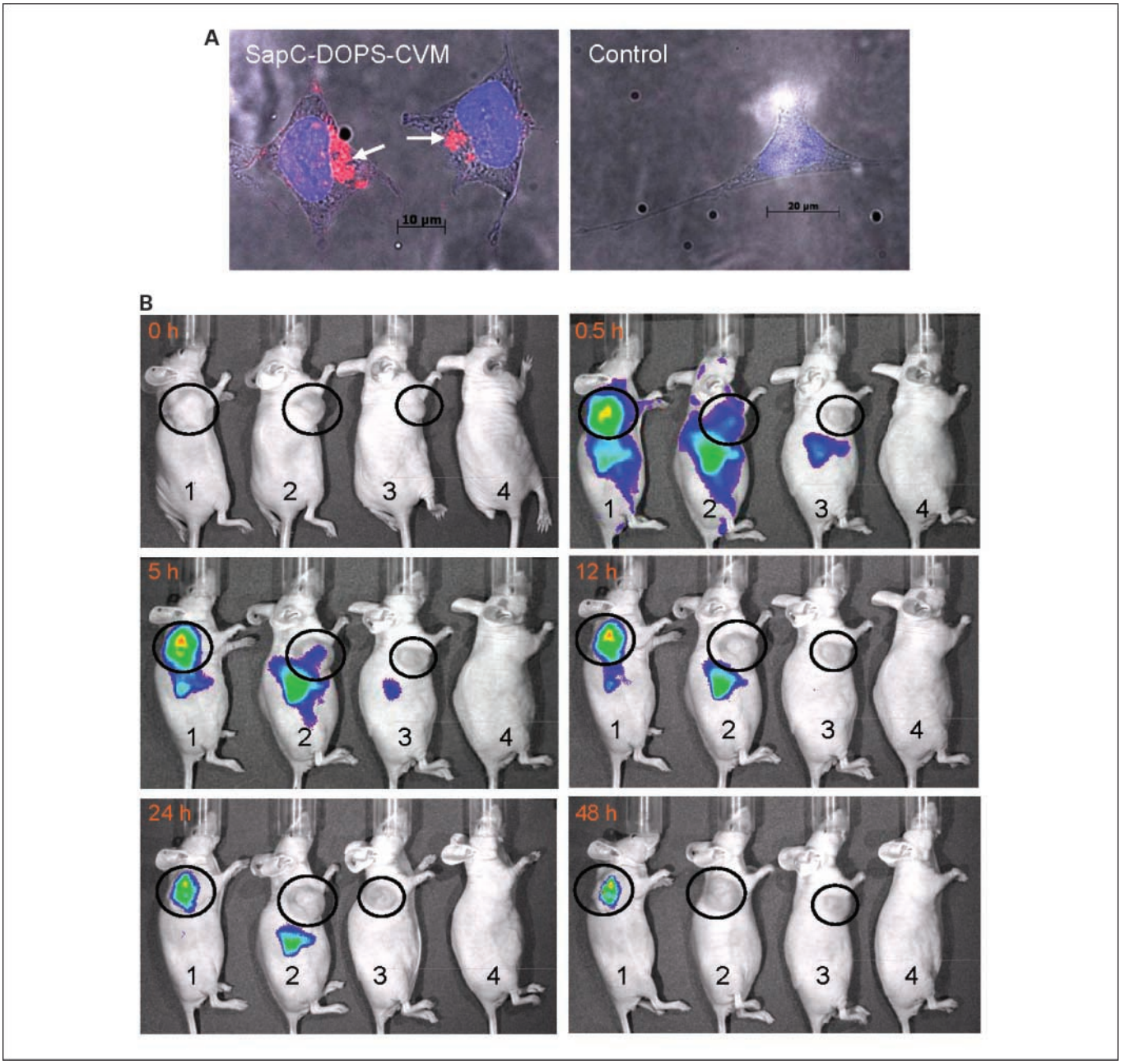

Fig. 4. Tumor targeting of fluorescent-labeled saposin C–dioleoylphosphatidylserine nanovesicles *in vitro* and *in vivo*. *A*, internalization of the CellVue Maroon–labeled saposin C–dioleoylphosphatidylserine in human neuroblastoma cells (CHLA-20). *B*, biodistribution of i.v. administered CellVue Maroon–labeled saposin C–dioleoylphosphatidylserine to mice bearing neuroblastoma xenografts indicates tumor-targeting potential. Athymic nude mice bearing neuroblastoma xenografts (*circled*) were treated with (from left to right) coupled CellVue Maroon–labeled saposin C–dioleoylphosphatidylserine nanovesicles (*1*), uncoupled saposin C and CellVue Maroon–labeled dioleoylphosphatidylserine vesicles (*2*), CellVue Maroon–labeled dioleoylphosphatidylserine vesicles alone (*3*), or PBS (*4*) in non–tumor bearing animals. Imaging time points were 0, 0.5, 5, 12, 24, and 48 h postinjection. Scale bars, 10 μm in (*A, left*); 20 μm in (*A, right*). Saposin C, 4.2 mg/kg; dioleoylphosphatidylserine, 2 mg/kg; CellVue Maroon, 6 μmol.

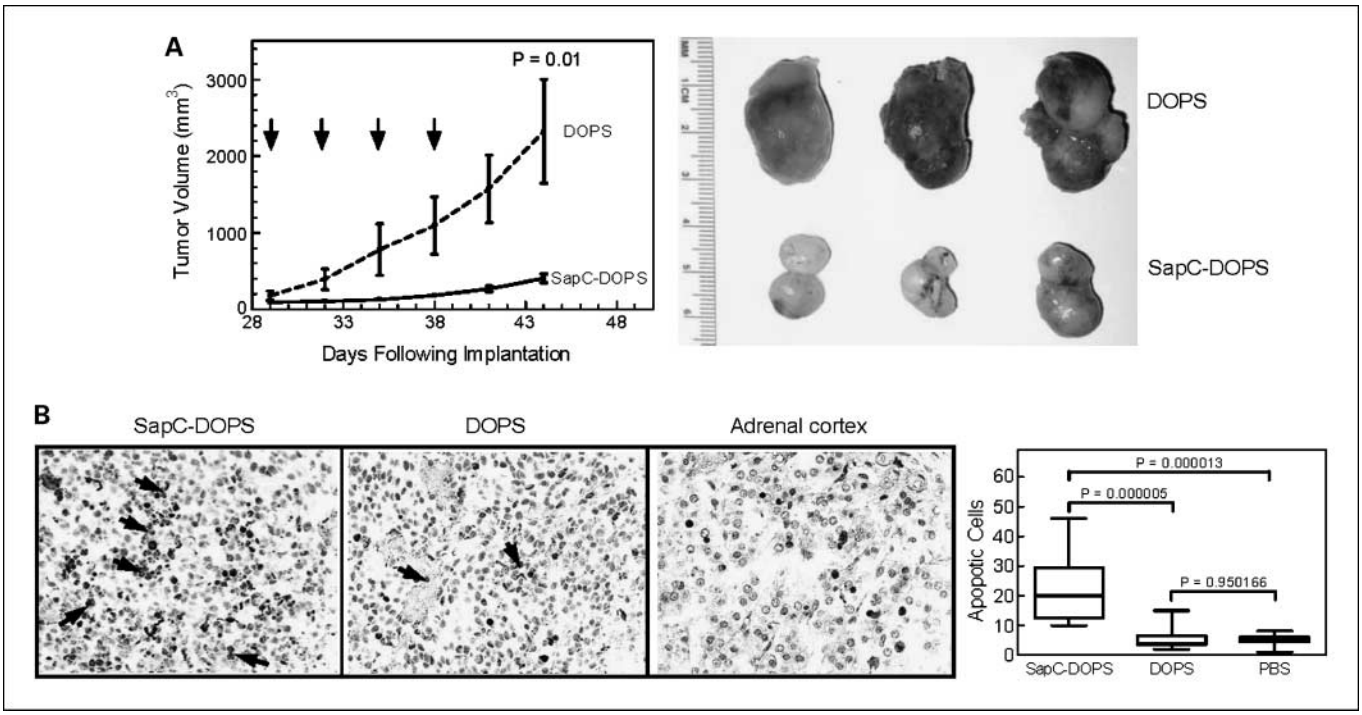

Fig. 5. Treatment of tumor-bearing mice with saposin C–dioleoylphosphatidylserine reduces tumor burden. *A,* athymic nude mice bearing s.c. neuroblastoma (CHLA-20) xenografts were treated with four doses of i.v. administered saposin C (8.4 mg/kg)–dioleoylphosphatidylserine (4 mg/kg) or dioleoylphosphatidylserine (4 mg/kg) by tail vein and followed for tumor growth (200 μL/injection). Saposin C–dioleoylphosphatidylserine treatment significantly inhibited tumor growth (*left*). Photograph of neuroblastoma (CHLA-20) tumor burden in saposin C–dioleoylphosphatidylserine or PBS-treated mice (*right*). *B,* tumor tissue from saposin C–dioleoylphosphatidylserine–treated animals contained abundant apoptotic cells by TUNEL staining (*pink* or *brown*) compared with animals treated with dioleoylphosphatidylserine alone. Original magnification, ×200. Quantitation of apoptotic cells from tumor sections of neuroblastoma (CHLA-20) xenografts as treated in (*B*). Apoptotic cells were counted in randomly selected field of view (10 per group).

saposin C–dioleoylphosphatidylserine complexes showed a linear correlation between fluorescence and dose (Supplementary Fig. S8A). In an experiment to assess tumor targeting efficiency following systemic administration, tumor-bearing mice were injected once with CellVue Maroon–labeled saposin C–dioleoylphosphatidylserine through the tail vein, and the fluorescence in tumors was quantified using the IVIS200 bioluminescence imaging system. At 24 hours postinjection, two groups of tumor-bearing mice showed tumor uptake efficiency at 39% to 43% (Supplementary Fig. S8B).

In vivo *antitumor efficacy of saposin C–dioleoylphosphatidylserine nanovesicles.* We evaluated the preclinical anticancer efficacyof saposin C–dioleoylphosphatidylserine against human neuroblastoma and malignant peripheral nerve sheath tumor xenografts. Mice bearing neuroblastoma xenografts were treated i.v. with saposin C–dioleoylphosphatidylserine or dioleoylphosphatidylserine alone, and tumor growth was observed over time. Animals receiving saposin C–dioleoylphosphatidylserine showed significant inhibition of tumor growth compared with the dioleoylphosphatidylserine treated group (Fig. 5A). The dose of saposin C and dioleoylphosphatidylserine in animal treatment studies through i.v. administration was 8.4 and 4 mg/kg in a total volume of 200 μL. Based on the optimal formulation concentration, this dose is the maximum feasible dose using the maximal volume possible for i.v. administration in a mouse. This mouse model allowed us to determine *in vivo* apoptotic cancer cell death induced by saposin C–dioleoylphosphatidylserine. Apoptotic cells were visualized by TUNEL assay in tumor tissues from mice treated with i.v. saposin C–dioleoylphosphatidylserine. Saposin C–dioleoylphosphatidylserine treated tumor tissues showed significantly increased numbers of apoptotic cells (~20 to 30 cells per field of view) compared with mice treated with dioleoylphosphatidylserine alone or PBS controls (~5 cells per field of view) in randomly selected imaging fields (Fig. 5B). Therefore, saposin C–dioleoylphosphatidylserine induced apoptosis was observed *in vitro* and *in vivo*.

Antitumor activity of saposin C–dioleoylphosphatidylserine was also evaluated against an i.p. xenograft model of human malignant peripheral nerve sheath tumor. Athymic nude mice bearing i.p. malignant peripheral nerve sheath tumor burden were treated with an i.p. injection of saposin C–dioleoylphosphatidylserine at 7, 10, 13, 16, 19, and 22 days post–cell implantation. By day 23, PBS-treated mice seemed cachectic and showed signs of gross tumor burden, whereas saposin C–dioleoylphosphatidylserine–treated mice showed minimal, if any, symptoms (Fig. 6A). Quantification of tumor burden revealed that saposin C–dioleoylphosphatidylserine treatment reduced tumor weight and nodule count by 50% at day 42 in this model (Fig. 6B). Overall, our experiment showed that saposin C–dioleoylphosphatidylserine had antitumor activity against preclinical models of human neuroblastoma and malignant peripheral nerve sheath tumor.

Preclinical study on saposin C–dioleoylphosphatidylserine toxicity. *In vivo* pharmacologic safety studies indicated that administration of saposin C–dioleoylphosphatidylserine at concentrations far higher than the therapeutic dose (4 mg/kg of

saposin C and 2 mg/kg of phosphatidylserine) caused no acute toxicity or pathologic symptoms (i.v. 12-fold higher or i.p. 36-fold higher). No weight loss was manifested in the saposin C–dioleoylphosphatidylserine treatment groups (Supplementary Fig. S9A). Histologic examination of the lung, liver, spleen, kidney, heart, and brain were evaluated by hematoxylin and eosin (H&E) staining (Supplementary Fig. S9B). No gross evidence of peritoneal inflammation, peritonitis, bowel obstruction, peristalsis of the intestines or stomach, and any obvious toxic effects on any peritoneal organs were observed. Overall, pathologic signs were not observed in any tissue sections from saposin C–dioleoylphosphatidylserine treated animals by either route.

Chronic toxicity studies were also carried out in FVB mice with a 2-fold concentration higher than the therapeutic dose. In these studies, animals were i.v. injected with saposin C (8 mg/kg) and dioleoylphosphatidylserine (4 mg/kg) once per week for 4 weeks. After 5 weeks, no weight lost was manifested in the saposin C–dioleoylphosphatidylserine treatment group (Supplementary Fig. S9C left), and no hematologic changes were observed (Supplementary Fig. S9C right). Histologic examination of the lung, liver, spleen, kidney, heart, spine, sciatic nerve, and brain was evaluated by H&E staining (Supplementary Fig. S9D). There were no inflammatory infiltrates in the portal areas of the liver and no evidence of hepatocellular degeneration. The spleen was histologically unremarkable. There were no degenerative changes in the neuronal population in the brain or evidence of gliosis or necrosis. There were no inflammatory infiltrates and no evidence of single cell necrosis. Sections of the lung showed no inflammatory infiltrates in the bronchial epithelium and no evidence of pneumonia or interstitial fibrosis. No evidence of myocardial necrosis or fibrosis was found in the heart. These experiments indicate that saposin C–dioleoylphosphatidylserine has no chronic toxicity.

Discussion

We have shown that saposin C–dioleoylphosphatidylserine nanovesicles specifically target tumor sites in preclinical animal models following systemic administration and that saposin C is essential for this process. Saposin C and dioleoylphosphatidylserine are naturally assembled to a monodispersed unilamellar nanovesicle. Saposin C–dioleoylphosphatidylserine nanovesicles readily extravasated into tumor tissues following i.v. administration, likely because of leaky tumor vasculature (41). Most importantly, saposin C–dioleoylphosphatidylserine nanovesicles accumulated and remained within tumor tissue for >48 hours. These results suggest that the phosphatidylserine lipid surface and acidic microenvironment of tumor tissues provide optimal conditions for the membrane fusogenic activity of saposin C. Saposin C–dioleoylphosphatidylserine nanovesicles are likely not only capable of passive transport into tumor tissue but are specifically retained in the tumor. The specific tumor-targeting property of saposin C–dioleoylphosphatidylserine nanovesicles may be exploited for the development of a robust delivery system for therapeutics.

In addition to specific tumor-targeting activity, saposin C–dioleoylphosphatidylserine nanovesicles are selectively cytotoxic for cancer cells. Our results show that saposin C–dioleoylphosphatidylserine induced apoptotic death of human cancer cells *in vitro* and *in vivo*. This induction was blocked by the addition of sphingomyelinase inhibitors. Remarkable elevation of ceramides detected in saposin C–dioleoylphosphatidylserine–treated cancer cells suggests that ceramide is a major mediator for the antineoplastic effect of saposin C–dioleoylphosphatidylserine. Sphinganine and sphingosine were significantly up-regulated, suggesting that these lipids may also participate in saposin C–dioleoylphosphatidylserine–mediated cell death. These sphingolipids are known to induce apoptosis in human cancer cells, including breast and rhabdomyosarcoma, through caspases (42, 43). This is an intriguing finding because saposin C–dioleoylphosphatidylserine may induce apoptosis through elevation of multiple sphingolipids. Overall, these data prove that saposin C–dioleoylphosphatidylserine is a novel cytotoxic agent targeting cancer cell membrane lipids.

Susceptibility of cells to apoptosis is influenced by the expression of a variety of genes and may especially be altered during transformation. An important regulator of apoptosis induction is the tumor suppressor protein p53, which is commonly

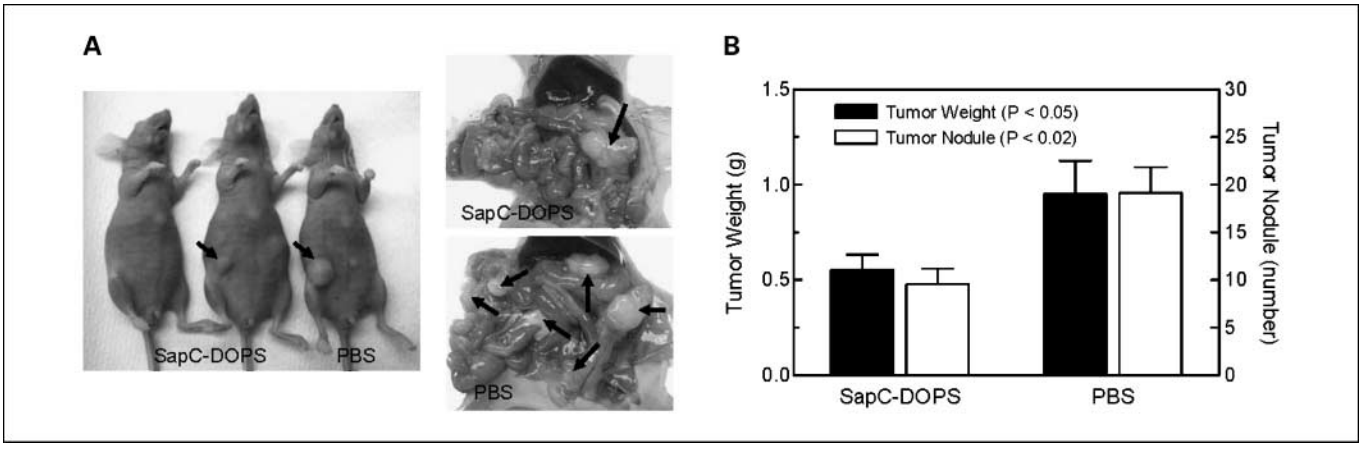

Fig. 6. Treatment of tumor-bearing mice with saposin C–dioleoylphosphatidylserine reduces tumor burden. *A,* photograph of malignant peripheral nerve sheath tumor burden in saposin C–dioleoylphosphatidylserine– or PBS-treated mice (*arrows*). *B,* comparison of tumor weight and nodule counts from saposin C–dioleoylphosphatidylserine– and PBS-treated mice. Tumors were collected 3 d after the last treatment. Every 3 d per injection for six injections (800 μL/injection): first dose, 33.6 mg/kg saposin C and 16 mg/kg dioleoylphosphatidylserine; second to sixth doses, 16.8 mg/kg saposin C and 8 mg/kg dioleoylphosphatidylserine.

mutated in many human cancer cells (44–46). Similarly, genes encoding other major mediators of apoptotic pathways are partially or completely deficient in a variety of human tumors and cell lines. For example, caspase-8 and caspase-3 are silenced in most human neuroblastoma (47–49) and breast cancer cells (50). Because saposin C–dioleoylphosphatidylserine induces apoptotic cell death of neuroblastoma and MCF-7 cells, this process is likely not dependent upon p53, caspase-3, or caspase-8. Alternatively, MCF-7 cells transfected with a dominant negative *caspase-9* gene were completely protected from the induction of apoptosis by saposin C–dioleoylphosphatidylserine. This finding suggests that caspase-9 is the major mediator in the saposin C–dioleoylphosphatidylserine–induced apoptotic pathway. To date, no cancer cells are reported to have caspase-9 defects, implicating widespread applicability for saposin C–dioleoylphosphatidylserine therapy.

Multidrug resistance is frequently seen in neuroblastoma and malignant peripheral nerve sheath tumor patients treated with chemotherapeutics. Resistance to these agents is often mediated through resistance to apoptosis as a result of overexpression of drug resistance genes (i.e., P-glycoprotein) or an inactivating mutation in one or more of the many component molecules of an apoptotic pathway. Saposin C–dioleoylphosphatidylserine showed cytotoxicity against several human neuroblastoma lines with positive multidrug resistance status, suggesting that saposin C–dioleoylphosphatidylserine–mediated induction of apoptosis is not dependent on these genes. Therefore, saposin C–dioleoylphosphatidylserine may offer an alternative for cancer patients whose tumors are unresponsive to conventional chemotherapy.

The immediate extracellular environment of tumor tissues commonly harbors sphingomyelinase resulting from tumor cell membrane leakiness. In addition, the acidic microenvironment of tumor cells favors the activity of saposin C preferentially as compared with normal tissues and cells. *In vivo* imaging with tumor-bearing mice showed that saposin C–dioleoylphosphatidylserine nanovesicles accumulated in tumor tissues and was cleared from normal tissues. Lack of *in vitro* toxicity and rapid turnover *in vivo* of saposin C–dioleoylphosphatidylserine in normal cells and tissues suggest its safety. These preclinical acute and chronic toxicity studies in immunocompetent mice show striking absence of toxicity and adverse side effects with use of saposin C–dioleoylphosphatidylserine.

In summary, saposin C–dioleoylphosphatidylserine nanovesicles are a novel anticancer agent that displays broad anticancer efficacy *in vitro* and *in vivo*. Our data support the notion that saposin C–dioleoylphosphatidylserine kills cancer cells at least in part through the accumulation of ceramides, leading to caspase activation and apoptotic cell death. Preferential tumor accumulation of saposin C–dioleoylphosphatidylserine results from its selective targeting to membrane lipids in the acidic microenvironment of tumors. Preclinical toxicity studies suggest a high clinical safety margin for saposin C–dioleoylphosphatidylserine. Therefore, saposin C–dioleoylphosphatidylserine nanovesicles have the potential to offer a targeted, potent, broad, and safe therapeutic agent for cancer patients.

Disclosure of Potential Conflicts of Interest

No potential conflicts of interest were disclosed.

Acknowledgments

We thank Drs. R. Jackson, R. Takigiku, and N. Robinson for the comments on the manuscript; Drs. C. Reynolds, Y. Lazebnik, and J. Li for the human cancer cell lines; C. Woods, M. Rolfes, and M. Taylor for the technical help; and the Lipidomics Core in the Medical University of South Carolina for the liquid chromatography–mass spectrometry analysis.

References

1. Sandhoff K, Kolter T, Harzer K. Sphingolipid activator proteins. In: Scriver CR, Beaudet AL, Sly WS, Valle D, editors. The metabolic and molecular bases of inherited disease. 8th ed. New York: McGraw-Hill, Inc.; 2000, p. 3371–88.
2. Qi X, Leonova T, Grabowski GA. Functional human saposins expressed in *Escherichia coli*. Evidence for binding and activation properties of saposins C with acid β-glucosidase. J Biol Chem 1994;269:16746–53.
3. Hiraiwa M, Soeda S, Martin BM, et al. The effect of carbohydrate removal on stability and activity of saposin B. Arch Biochem Biophys 1993;303:326–31.
4. Qi X, Chu Z. Fusogenic domain and lysines in saposin C. Arch Biochem Biophys 2004;424:210–8.
5. Qi X, Qin W, Sun Y, Kondoh K, Grabowski GA. Functional organization of saposin C. Definition of the neurotrophic and acid β-glucosidase activation regions. J Biol Chem 1996;271:6874–80.
6. Harzer K, Paton BC, Christomanou H, et al. Saposins (sap) A and C activate the degradation of galactosylceramide in living cells. FEBS Lett 1997;417:270–4.
7. Linke T, Wilkening G, Lansmann S, et al. Stimulation of acid sphingomyelinase activity by lysosomal lipids and sphingolipid activator proteins. Biol Chem 2001;382:283–90.
8. Morimoto S, Yamamoto Y, O'Brien JS, Kishimoto Y. Distribution of saposin proteins (sphingolipid activator proteins) in lysosomal storage and other diseases. Proc Natl Acad Sci U S A 1990;87:3493–7.
9. Qi X, Grabowski GA. Differential membrane interactions of saposins A and C: implications for the functional specificity. J Biol Chem 2001;276:27010–7.
10. Hiraiwa M, Soeda S, Kishimoto Y, O'Brien JS. Binding and transport of gangliosides by prosaposin. Proc Natl Acad Sci U S A 1992;89:11254–8.
11. You HX, Yu L, Qi X. Phospholipid membrane restructuring induced by saposin C: a topographic study using atomic force microscopy. FEBS Lett 2001;503:97–102.
12. Vaccaro AM, Tatti M, Ciaffoni F, Salvioli R, Serafino A, Barca A. Saposin C induces pH-dependent destabilization and fusion of phosphatidylserine-containing vesicles. FEBS Lett 1994;349:181–6.
13. You HX, Qi X, Grabowski GA, Yu L. Phospholipid membrane interactions of saposin C: *in situ* atomic force microscopic study. Biophys J 2003;84:2043–57.
14. Wang Y, Grabowski GA, Qi X. Phospholipid vesicle fusion induced by saposin C. Arch Biochem Biophys 2003;415:43–53.
15. Ran S, Thorpe PE. Phosphatidylserine is a marker of tumor vasculature and a potential target for cancer imaging and therapy. Int J Radiat Oncol Biol Phys 2002;54:1479–84.
16. Utsugi T, Schroit AJ, Connor J, Bucana CD, Fidler IJ. Elevated expression of phosphatidylserine in the outer membrane leaflet of human tumor cells and recognition by activated human blood monocytes. Cancer Res 1991;51:3062–6.
17. Vaupel P, Kallinowski F, Okunieff P. Blood flow, oxygen and nutrient supply, and metabolic microenvironment of human tumors: a review. Cancer Res 1989;49:6449–65.
18. Wike-Hooley JL, Haveman J, Reinhold HS. The relevance of tumour pH to the treatment of malignant disease. Radiother Oncol 1984;2:343–66.
19. Wallach DF. Generalized membrane defects in cancer. N Engl J Med 1969;280:761–7.
20. Wallach DF. Cellular membrane alterations in neoplasia: a review and a unifying hypothesis. Curr Top Microbiol Immunol 1969;47:152–76.
21. Wallach DF. Membrane biology and cancer therapy. Pathobiol Annu 1978;8:189–216.
22. Allison AC. Lysosomes in cancer cells. J Clin Pathol Suppl (R Coll Pathol) 1974;7:43–50.
23. Boyer MJ, Tannock IF. Lysosomes, lysosomal enzymes, and cancer. Adv Cancer Res 1993;60:269–91.
24. Unger C. Current concepts of treatment in medical oncology: new anticancer drugs. J Cancer Res Clin Oncol 1996;122:189–98.
25. Hendrich AB, Michalak K. Lipids as a target for drugs modulating multidrug resistance of cancer cells. Curr Drug Targets 2003;4:23–30.

26. Chalfant CE, Rathman K, Pinkerman RL, et al. *De novo* ceramide regulates the alternative splicing of caspase 9 and Bcl-x in A549 lung adenocarcinoma cells. Dependence on protein phosphatase-1. J Biol Chem 2002;277:12587–95.
27. Erdreich-Epstein A, Tran LB, Bowman NN, et al. Ceramide signaling in fenretinide-induced endothelial cell apoptosis. J Biol Chem 2002;277: 49531–7.
28. Kilkus J, Goswami R, Testai FD, Dawson G. Ceramide in rafts (detergent-insoluble fraction) mediates cell death in neurotumor cell lines. J Neurosci Res 2003;72:65–75.
29. Ditaranto-Desimone K, Saito M, Tekirian TL, et al. Neuronal endosomal/lysosomal membrane destabilization activates caspases and induces abnormal accumulation of the lipid secondary messenger ceramide. Brain Res Bull 2003;59:523–31.
30. Schmidt ML, Lukens JN, Seeger RC, et al. Biologic factors determine prognosis in infants with stage IV neuroblastoma: a prospective Children's Cancer Group study. J Clin Oncol 2000;18: 1260–8.
31. Izbicki T, Mazur J, Izbicka E. Epidemiology of neuroblastoma: analysis of a single institution. Anticancer Res 2003;23:1933–8.
32. Theos A, Korf BR. Pathophysiology of neurofibromatosis type 1. Ann Int Med 2006;144:842–9.
33. Keshelava N, Seeger RC, Groshen S, Reynolds CP. Drug resistance patterns of human neuroblastoma cell lines derived from patients at different phases of therapy. Cancer Res 1998;58: 5396–405.
34. Komdeur R, Plaat BE, van der Graaf WT, et al. Expression of multidrug resistance proteins, P-gp, MRP1 and LRP, in soft tissue sarcomas analysed according to their histological type and grade. Eur J Cancer 2003;39:909–16.
35. Sharif S, Ferner R, Birch JM, et al. Second primary tumors in neurofibromatosis 1 patients treated for optic glioma: substantial risks after radiotherapy. J Clin Oncol 2006;24:2570–5.
36. Mahller YY, Vaikunth SS, Currier MA, et al. Oncolytic HSV and erlotinib inhibit tumor growth and angiogenesis in a novel malignant peripheral nerve sheath tumor xenograft model. Mol Ther 2007;15:279–86.
37. Chu Z, Sun Y, Kuan CY, Grabowski GA, Qi X. Saposin C: neuronal effect and CNS delivery by liposomes. Ann N Y Acad Sci 2005;1053:237–46.
38. Liu B, Hannun YA. Sphingomyelinase assay using radiolabeled substrate. Methods Enzymol 2000;311:164–7.
39. Bielawski J, Szulc ZM, Hannun YA, Bielawska A. Simultaneous quantitative analysis of bioactive sphingolipids by high-performance liquid chromatography-tandem mass spectrometry. Methods 2006;39:82–91.
40. Perry DK, Bielawska A, Hannun YA. Quantitative determination of ceramide using diglyceride kinase. Methods Enzymol 2000;312:22–31.
41. Allen TM, Cullis PR. Drug delivery systems: entering the mainstream. Science 2004;303:1818–22.
42. Ahn EH, Chang CC, Schroeder JJ. Evaluation of sphinganine and sphingosine as human breast cancer chemotherapeutic and chemopreventive agents. Exp Biol Med 2006;231: 1664–72.
43. Phillips DC, Martin S, Doyle BT, Houghton JA. Sphingosine-induced apoptosis in rhabdomyosarcoma cell lines is dependent on pre-mitochondrial Bax activation and post-mitochondrial caspases. Cancer Res 2007;67:756–64.
44. Greenblatt MS, Bennett WP, Hollstein M, Harris CC. Mutations in the *p53* tumor suppressor gene: clues to cancer etiology and molecular pathogenesis. Cancer Res 1994;54:4855–78.
45. Harris CC. The 1995 Walter Hubert Lecture—molecular epidemiology of human cancer: insights from the mutational analysis of the *p53* tumour-suppressor gene. Br J Cancer 1996;73:261–9.
46. Hollstein M, Sidransky D, Vogelstein B, Harris CC. p53 Mutations in human cancers. Science 1991;253:49–53.
47. Hopkins-Donaldson S, Bodmer JL, Bourloud KB, Brognara CB, Tschopp J, Gross N. Loss of caspase-8 expression in neuroblastoma is related to malignancy and resistance to TRAIL-induced apoptosis. Med Pediatr Oncol 2000;35:608–11.
48. Eggert A, Grotzer MA, Zuzak TJ, et al. Resistance to tumor necrosis factor-related apoptosis-inducing ligand (TRAIL)-induced apoptosis in neuroblastoma cells correlates with a loss of caspase-8 expression. Cancer Res 2001;61:1314–9.
49. Teitz T, Lahti JM, Kidd VJ. Aggressive childhood neuroblastomas do not express caspase-8: an important component of programmed cell death. J Mol Med 2001;79:428–36.
50. Janicke RU, Sprengart ML, Wati MR, Porter AG. Caspase-3 is required for DNA fragmentation and morphological changes associated with apoptosis. J Biol Chem 1998;273:9357–60.